ORIGINAL PAPER

On the Suitability of NO_x-Storage-Catalysts for Hydrogen Internal Combustion Engines and a Radio Frequency-Based NO_x Loading Monitoring

S. Walter[1] · G. Hagen[1] · D. Koch[2] · A. Geißelmann[3] · R. Moos[1]

Abstract

Hydrogen combustion engines can contribute to CO_2-free mobility. However, they produce NO_x emissions, albeit only to an extremely small extent when operated very leanly. One approach to reduce these emissions even further is to use exhaust gas aftertreatment systems like NO_x storage catalysts (NSC). So far, they have mainly been used in diesel or gasoline applications. This contribution shows that under conditions such as those prevailing in hydrogen engines, the NSC can achieve not only a higher storage capacity for nitrogen oxides (NO_x) but also a higher conversion. To ensure permanently high conversion rates, the amount of stored NO_x has to be monitored permanently to prevent NO_x breakthroughs. Conventional NO_x sensors may not be accurate enough due to the very low NO_x emissions. The functionality of the radio frequency (RF) sensor, which enables a direct determination of the NO_x loading, is demonstrated for operation under hydrogen conditions. Furthermore, the influence of rich exhaust gas on the RF signal, which is relevant for a correct NO_x loading determination during regeneration, is analyzed.

1 Introduction

Besides the ongoing tightening of exhaust emission limits, e.g. with regard to nitrogen oxides, the urgency to reduce global CO_2 emissions poses major challenges for the future usage of combustion engines. In 2010, the transport sector contributed a total of 14% to the global greenhouse gas emissions [1]. Primary contributors are road vehicles, which account for 72% of these emissions [2]. Thus, to achieve the desired CO_2 reduction targets, conventional combustion engine vehicles using non-renewable fossil fuels have to be replaced. Currently, this is mainly accomplished by battery electric vehicles. Due to numerous challenges, such as short range along with long charging times, the establishment of the charging infrastructure or the impact of charging on the power grid, "clean" fuels can be an alternative [3–5].

"Clean" fuel refers to carbon–neutral fuels, that are produced using renewable energy. One example thereof is hydrogen (H_2), which can be used in fuel cells, to generate electrical energy, or directly in internal combustion engines (ICE) [6–8]. Hydrogen fueled ICEs (H_2-ICE) offer a number of advantages, such as lower required fuel purity or simpler manufacturing process [9]. Furthermore, nitrogen oxides (NO_x) can be formed by the Zeldovich mechanism due to high combustion temperatures, albeit to a much lesser extent compared to conventional combustion engines when operated very leanly [9–12]. Therefore, to achieve a zero emission vehicle, an exhaust gas aftertreatment system is necessary for H_2-ICEs [13, 14]. One option is the selective catalytic reduction (SCR), which is one of the major exhaust aftertreatment technologies in diesel applications [15]. These catalysts require a reductant in the form of ammonia (NH_3) to convert nitrogen oxides. That must be provided separately, e.g. in form of an aqueous urea solution.

✉ S. Walter
  Functional.Materials@uni-bayreuth.de

1   Department of Functional Materials, Bayreuth Engine Research Center (BERC), University of Bayreuth, 95440 Bayreuth, Germany

2   Keyou GmbH, 80335 Munich, Germany

3   Umicore AG & Co. KG, Rodenbacher Chaussee 4, 63457 Hanau-Wolfgang, Germany

To avoid this, some approaches utilize the already available hydrogen fuel as the reducing agent (H_2-SCR). However, this goes along with significantly lower conversion rates than conventional SCR systems [13, 16–19].

An alternative solution for catalytic exhaust gas aftertreatment are NO_x storage catalysts (NSC). They store nitrogen oxides under lean exhaust gas conditions and reduce them subsequently during a short rich phase [20]. In addition to the nitrogen oxide storage, NSCs usually contain ceria for oxygen storage [21]. In detail, NO in the exhaust must first be oxidized at catalytically active platinum sites (Eq. 1) [22].

$$2\,NO\,+\,O_2\,\rightarrow\,2\,NO_2 \tag{1}$$

Subsequently, it is stored as nitrate by converting the carbonates of the storage material while releasing CO_2 (e.g. Eq. 2 with a barium based storage material) [23].

$$2\,BaCO_3 + 2\,NO_2 + 1/2\,O_2 \leftrightarrow Ba\left(NO_3\right)_2 + CO_2 \tag{2}$$
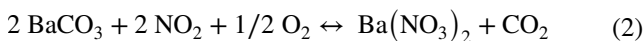
Under rich conditions reducing exhaust components convert the stored NO_x to harmless gases, like H_2O and N_2. Thereby, hydrogen is considered the most effective reducing agent [23, 24]. Consequently, the regeneration behavior of the NSC with a H_2-ICE should not be worse or even better than with a diesel engine, regardless of the lower CO_2 concentration in the exhaust gas originating only from the intake air.

According to Eq. 2, CO_2 must be present to restore the carbonate state of the storage material during releasing nitrogen oxides. In a hydrogen engine, however, CO_2 is limited to the fraction already present in the intake air and, to a very small extent, to burnt engine oil [25]. Nevertheless, a release of nitrogen oxides is possible despite low CO_2 concentrations, whereby the storage material is then not present as a carbonate but as hydroxide [e.g. $Ba(OH)_2$] or oxide (e.g. BaO) [26, 27]. Conversion to one of these compounds in an almost CO_2-free atmosphere could even have a positive effect on the NO_x storage capacity [27]. This paper will examine whether this effect can also be found in commercially available NSCs during exhaust gas conditions comparable to H_2-ICEs. Furthermore, the conversion performance of an NSC under "hydrogen conditions" as well as its selectivity will also be analyzed and compared with those in a typical diesel engine application.

In addition, the engine operation regarding to air–fuel ratio has be controlled depending on the NO_x loading [28]. This is usually determined by cumulative balancing of NO_x concentration signals from NO_x sensors up- and downstream of the catalyst [29]. Due to up to two magnitudes lower concentrations in lean-operated hydrogen engines than in typical diesel engines, this is, however, strongly dependent on the accuracy of the sensors [10]. The accuracy of a typical NO_x sensor is ± 10 ppm for NO < 100 ppm ($\pm 10\%$

above 100 ppm) [30]. An alternative approach is the radio frequency (RF) based catalyst state diagnosis (RF-sensor). It determines the loading state directly by measuring the dielectric properties of the storage material [31, 32]. The functionality of the RF-sensor has already been demonstrated for NSCs with diesel engines [33, 34]. Additionally, this work will investigate whether monitoring of the NO_x loading via the RF-sensor is still possible for the exhaust gas conditions of a hydrogen engine and how the RF-signal depends on the air–fuel ratio during regeneration.

2 RF Catalyst State Diagnosis

The RF-sensor can detect the state of a catalyst via the propagation behavior of electromagnetic waves within the catalyst. They depend on the dielectric properties of the catalyst [31, 35]. For this purpose, the RF-sensor excites standing electromagnetic waves (resonances) inside the metallic catalyst canning using two coupling elements in the form of coaxial probe antennas. These resonances can be evaluated with respect to characteristic parameters, like the resonant frequency f_{res} and the quality factor Q_0. Both parameters depend on the complex relative permittivity ($\underline{\varepsilon} = \varepsilon_1 - j\varepsilon_2$). Based on the cavity perturbation method, an increase in material polarization χ_e (resp. relative permittivity ε_1) results in a decrease of the resonant frequency (Eq. 3). The inverse quality factor Q_0^{-1}, on the other hand, is directly proportional to the dielectric losses ε_2 of the catalyst (Eq. 4) [35–37].

$$\Delta f_{res} \propto -\Delta\chi_e = -\Delta\left(\varepsilon_1 - 1\right) \tag{3}$$

$$\Delta Q_0^{-1} \propto \Delta\varepsilon_2 \tag{4}$$

However, the relationships described in Eqs. 3 and 4 apply only to small material samples compared to the resonant cavity (i.e., the canning). For larger samples, as a catalyst typically is, interference between the two resonant parameters may occur [37]. Nevertheless, it could have already been shown in [34], that these two effects allow a distinct evaluation of the storage components of an NSC. While oxygen storage mainly influences the quality factor, the amount of stored NO_x affects mainly the resonant frequency.
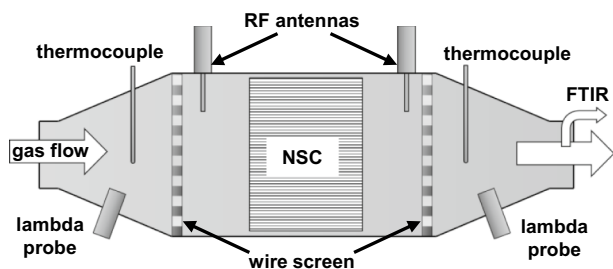
3 Experimental

In this work, a commercially available honeycomb NSC (kindly provided by Umicore) with a cell density of 400 cpsi and a precious metal content of 43 g/ft^3 platinum, 10 g/ft^3 palladium and 2 g/ft^3 rhodium was examined. Since all

measurements were performed on a gas test bench with a flow rate of 40 l/min, cores of 4.6 cm diameter and 2.54 cm length were cut from the NSC to obtain a space velocity of around 57,000 1/h, comparable to real engine conditions. The catalyst temperature was varied between 220 and 420 °C by adjusting the preheated gas mixture as well as an external heating of the canning to reduce heat losses. Gas temperature was measured using thermocouples up- and downstream of the catalyst. Their average is the catalyst temperature T_{NSC}. During lean gas conditions, the maximum temperature difference between both thermocouples was below 8 °C, and less than 1 °C under stationary rich conditions.

To determine the conversion characteristics of the NSC, a part of the downstream gas was analyzed by Fourier-transform infrared spectroscopy (FTIR). In addition, a broadband lambda probe was located up- and downstream, allowing for evaluation of the stored oxygen during regeneration. The lambda probe, however, is calibrated to typical diesel exhaust gas and therefore does not provide an accurate air–fuel ratio due to the rich-shift phenomena [38]. Nevertheless, it can be used to determine the point in time when the oxygen storage is completely emptied respectively filled. During all investigations, a vector network analyzer connected to both antennas was used to measure the complex scattering parameter S_{21} about every 0.6 s in the range from 3.55 to 3.70 GHz. From these data, the resonant frequency f_{res} and the quality factor Q_0 of the TE_{113} resonant mode were determined as described in [39]. The measurement setup is shown schematically in Fig. 1.

All experiments used nitrogen with 8 vol% water as base gas. To set exhaust gas conditions similar to a H_2-ICE, 0.1% CO_2 was added ("H_2 conditions"). In order to compare the catalyst performance under these conditions with that of a diesel engine, the tests were also carried out with 7% CO_2 ("diesel conditions"). Before each measurement, the NSC was preconditioned by several rich-lean changes. The rich phases were set for the "H_2 conditions" by solely adding hydrogen to the base gas, while for the diesel conditions,

carbon monoxide was present as well. The lean phases were realized regardless of engine operation by adding oxygen.

4 Results and Discussion

4.1 Influence of Rich Gas Atmospheres on the RF-Sensor

First, the influence of rich exhaust gas, in particular regarding the radio frequency signal, was determined. This analysis was carried out exclusively for conditions occurring with a H_2-ICE (i.e., at 0.1% CO_2). For this purpose, after a lean phase, rich conditions were set by adding 1% H_2 to the then oxygen-free base gas. After reaching stabilized gas concentrations downstream of the NSC, the hydrogen concentration was reduced stepwise to 0.7%, 0.5%, 0.2% and 0.1% before returning to lean atmosphere. This measurement is shown in Fig. 2 exemplarily for a gas temperature of about 370 °C. Thereby, the downstream air–fuel ratio measured with the lambda probe ranges from 0.935 to 0.996 and decreases with the reduction of the supplied hydrogen. Depending on this, also carbon monoxide forms, which can be explained by the reverse water gas shift reaction [40]. Due to the small amounts of CO_2 converted by this reaction, it has no measurable effect on CO_2. Significant changes, however, can be measured shortly after rich-lean changes. The short decrease in downstream CO_2 concentration can be explained by its sorption into the NSC storage material. In turn, switching
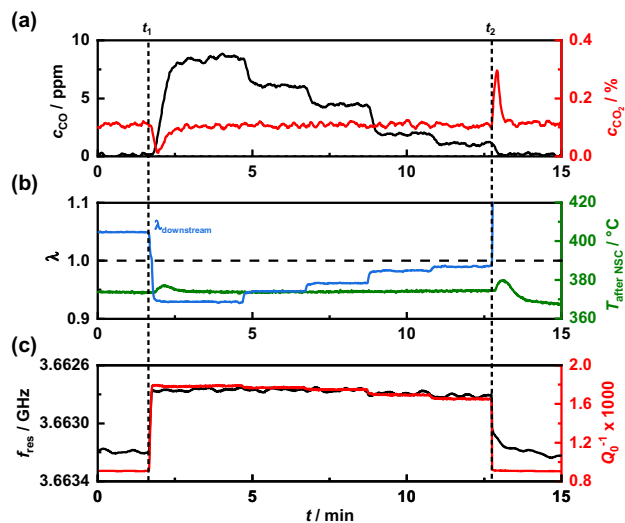

Fig. 1 Schematic illustration of the experimental setup. In addition to the canning, the resonant cavity is further defined by wire screens up- and downstream of the catalyst to increase the signal quality of the RF-sensor

Fig. 2 Variation of hydrogen content under rich exhaust gas conditions at around 370 °C; **a** downstream concentration of CO (black) and CO_2 (red) measured with FTIR; **b** λ (blue) and gas temperature (green) downstream of the NSC; **c** resonant frequency (black) and invers quality factor (red). The switch to rich conditions (t_1) as well as back to lean (t_2) are marked with dashed lines (Color figure online)

back to lean leads to the release of CO_2 over a period of only 30 s.

The resonant parameters also indicate the rapid transformation of the catalyst material after switching between rich and lean. In rich, the inverse quality factor Q_0^{-1} increases significantly, indicating higher dielectric losses according to Eq. 4. These losses may occur, for instance, not only due to sorption of CO_2, but also due to the oxidation state of the ceria [41]. Simultaneously, the resonant frequency f_{res} decreases. This can be explained by the higher permittivity in the oxidized state.

The differences in the resonant parameters compared between rich and lean was evaluated in a temperature range from 220 to 420 °C for each rich gas composition after reaching a steady state (Fig. 3). In case of the resonant frequency, it is noticeable that – independent of the air–fuel ratio—at low temperatures, a shift towards higher frequencies occurs, while above 300 °C the shift tends towards lower frequencies. A similar behavior was already observed in [34]. This could be an indication of the influence of different storage materials. An increase in resonant frequency should only be caused by a decrease in permittivity. However, it is known from [41] that the permittivity of ceria in the reduced state is always above the oxidized value. Thus, the increase in the resonant frequency is possibly due to a higher permittivity of the NO_x storage material. However, since the exact material composition of the studied NSC is not known, a change in oxygen storage cannot be excluded as a possible reason for the increase in resonant frequency, especially since even at the lowest examined temperatures, storage of oxygen by the storage material could still be observed by the lambda probes during the rich-lean changes.

Regarding the quality factor, the signal difference to lean increases significantly with higher temperatures, but is still noticeable at the lowest observed temperature of 220 °C. Therefore, the temperature-dependent behavior is strongly similar to that of pure ceria in a TWC [41]. With variation of hydrogen concentration respectively the reduction of richness level, changes in the resonant parameters occur, albeit to a minor extent compared to the change from lean to rich. In general, a richer gas mixture leads to a stronger change

of the resonant parameters. A similar behavior has already been observed for TWCs and could be associated with the oxidation degree of ceria [42].

4.2 Storage and Regeneration Behavior

In this section, NO_x sorption and the subsequent regeneration of the NSC will be examined. Thereby, conversion characteristics during a typical operation with a H_2-ICE will be compared to those with a diesel engine. Regarding "H_2 conditions", a lean gas mixture was set at the beginning of the experiment by adding 10% oxygen to the base gas (8% H_2O and 0.1% CO_2 in nitrogen). Subsequently, 40 ppm NO were added and the empty NSC got loaded with NO_x until a (almost) complete breakthrough of NO_x was reached. Then, regeneration was initiated by switching to rich gas, which was achieved by adding 1% hydrogen to the base gas. In chosen "diesel operation conditions", which refers to a base gas with 8% H_2O and 7% CO_2, NO_x storage took place at a lower oxygen content of 1% but at significantly higher NO concentration of 500 ppm. Regeneration occurred without hydrogen only by adding 0.4% carbon monoxide. The gas concentrations during these tests are summarized in Table 1.

The NO_x loading shown in Fig. 4 – just as the lambda variation in Fig. 2 – was carried out under "H_2 conditions" at a temperature of approx. 370 °C and lasted 80 min. Based on the measured NO_x concentrations up- respectively downstream (Fig. 4a), the amount of stored NO m_{NO} could be determined for all storage experiments (Fig. 4b) by integration. The resonant parameters are shown in Fig. 4c) with the same scaling as for the air–fuel ratio variation in Fig. 2. Thereby it can be clearly seen that the dielectric losses, described by the inverse quality factor, are barely affected

Table 1 Gas concentrations added to the base gas during the experiments to determine the storage and regeneration behavior of the NSC

	Lean operation	NO_x loading	Rich operation
"H_2"	10% O_2	40 ppm NO	1% H_2
"Diesel"	1% O_2	500 ppm NO	0.4% CO

Fig. 3 Temperature-dependent shift of resonant frequency Δf_{res} (**a**) and inverse quality factor ΔQ_0^{-1} (**b**) under different rich gas atmospheres compared to lean conditions
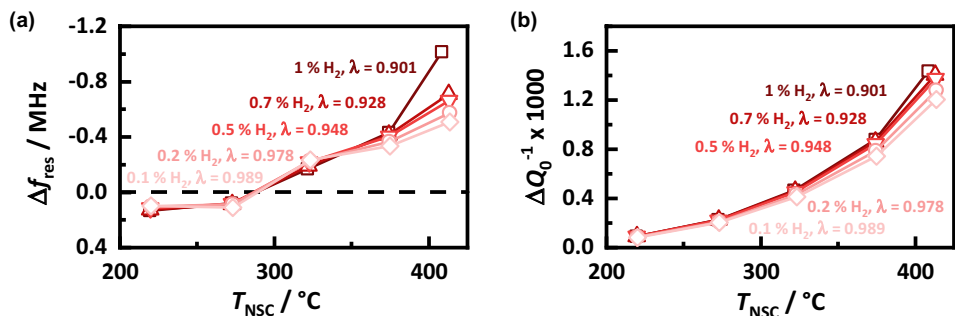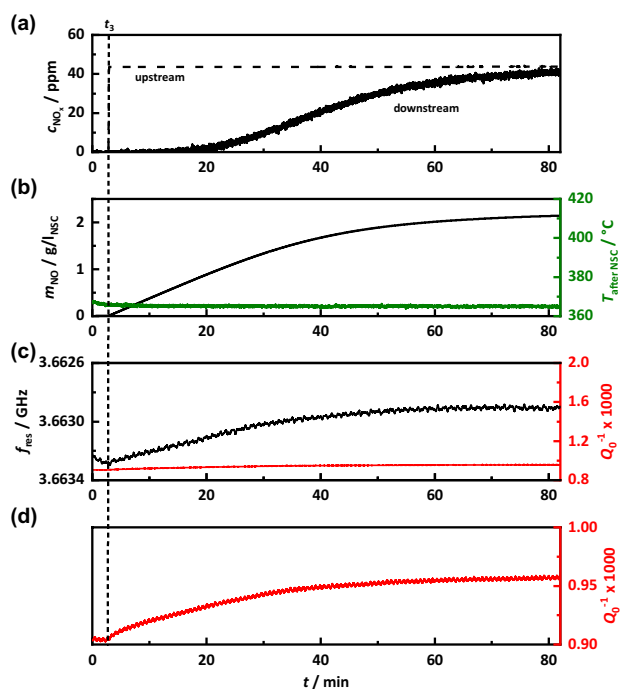
Fig. 4 NO_x storage under "hydrogen conditions" at around 370 °C. Start of NO admixture at t_3 is marked with a dotted line; **a** concentration of NO_x upstream (dashed line) and downstream of the catalyst; **b** calculated mass of NO stored in the NSC relative to its volume m_{NO} and gas temperature downstream the NSC (green); **c** resonant frequency (black) and invers quality factor (red) with the same axis scaling as in Fig. 2; **d** inverse quality factor (red) as in (**c**) but with different scaling (to highlight the small effect) (Color figure online)

by NO. Thus, a stored NO amount of 2 g/l_{NSC} yielded an increase of Q_0^{-1} by 0.05, while switching to rich conditions resulted in a 16 times greater increase (cf. Figure 2c). Despite the only small signal change, the quality factor nevertheless resembles the stored NO (Fig. 4d). In case of the resonant frequency, in contrast, the effect is much more pronounced compared to rich-lean changes. In addition, the resonant frequency clearly resembles the storage signal m_{NO}.

Examining the resonance parameter shift as a function of the stored NO mass m_{NO} in Fig. 5 confirms the linear relationship regardless of the catalyst temperature. However,
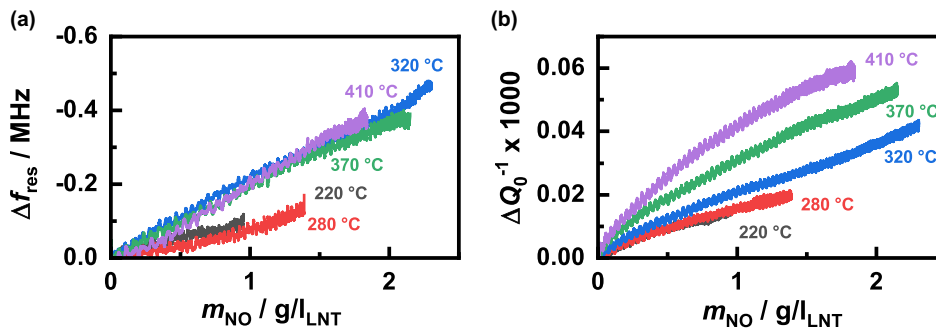
the sensitivity of the RF signal varies with the temperature significantly. The response of resonant parameters to NO loading during "H_2 conditions" is thus consistent with the findings in [34] and will therefore not be discussed further in this work.

The subsequent regeneration is considerably faster than the storage phase (Fig. 6). After just 1.5 min ($t > t_7$) after starting regeneration at t_4, barely any undesired by-products resulting from NO_x conversion, such as nitrous oxide (N_2O) or ammonia (NH_3), can be detected downstream. Also, for $t > t_7$, the downstream temperature has dropped to a steady state value after a brief peak of 40 K due to the exothermic regeneration. Initiating regeneration (t_4), the downstream air–fuel ratio does not immediately switch to rich in contrast to the value measured upstream, but remains at stoichiometric for about 30 s (until t_5) due to the consumption of oxygen stored in the NSC. This is mirrored by the inverse quality factor Q_0^{-1} that increases almost linearly during this period indicating ceria reduction as known from [43]. Evaluation of still stored NO is more difficult. On one hand, unlike during the sorption process, it cannot be determined by balancing gas concentrations before and after the catalyst, since hydrogen used for regeneration cannot be measured by FTIR. On the other hand, evaluation of the resonant frequency also turns out to be more difficult, since different material effects are overlapping as a result of simultaneous NO_x and oxygen release. Furthermore, the resonant frequency is also more dependent on temperature changes than the quality factor, which can be seen, for example, in its increase after t_8. This is due to a temperature decrease of the catalyst canning as there is no longer an additional heat source due to the exothermic reactions during the regeneration phase. The subsequent thermal reduction in size leads to a decreased resonant cavity size and thus to an increase in the resonant frequency. Nevertheless, after reaching an almost constant resonant frequency signal from t_6 onward, a completely emptied NO_x storage can be assumed, since at this point the oxygen storage is already completely reduced.

For easier comparison of the NO_x storage characteristics under different gas conditions simulating a hydrogen and diesel combustion engine, the stored NO shortly before
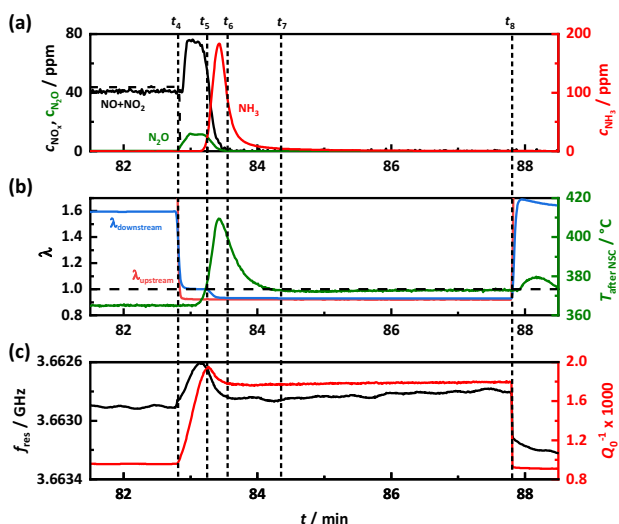
Fig. 5 Shift of resonant frequency Δf_{res} (**a**) and inverse quality factor ΔQ_0^{-1} (**b**) relative to the NSC under lean conditions depending on the amount of stored NO for different catalyst temperatures

Fig. 6 Regeneration under hydrogen conditions" at around 370 °C. Start of regeneration at t_4, end of stoichiometric conditions downstream at t_5, reaching a constant resonant frequency at t_6, reaching constant temperature at t_7 and change back to lean conditions at t_8 are marked with a dotted line; **a** concentration of NO upstream (dashed line) and NO+NO$_2$ (black) resp. N$_2$O (green) downstream of the catalyst on the left y-axis and downstream NH$_3$ concentration (red) on the right y-axis; **b** measured λ downstream (blue) and upstream (red) of the catalyst as well as gas temperature (green) downstream the NSC. The upstream lambda signal during lean phases deviates significantly from the downstream signal with a value of approx. 3.4 and is therefore not visible in the graph, as the scaling was chosen with a focus on the breakthrough behavior of the oxygen storage during the regeneration; **c** resonant frequency (black) and invers quality factor (red) with equal axis scaling as in Fig. 4 (Color figure online)

regeneration $m_{NO,max}$ (i.e., the maximum storable NO mass at the given gas conditions) was evaluated (Fig. 7a). At temperatures above 300 °C, approx. 50% more NO could be stored under the conditions prevailing at a H$_2$-ICE. A reason therefore could be due to the high oxygen levels under hydrogen conditions [44, 45]. At lower temperatures, storage capacity drops to the same level for both operating modes of about 1 g/l$_{NSC}$. However, even with this reduced storage ability, the NSC would still be able
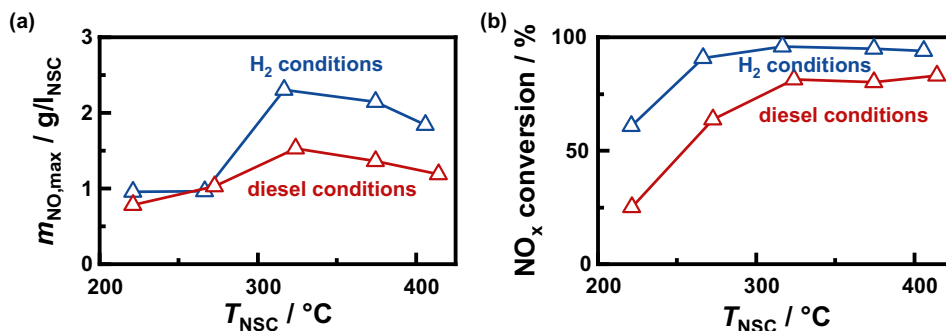
to buffer emissions of 40 ppm NO at a space velocity of 60,000 1/h over a period of 20 min.

The NO$_x$ conversion rates shown in Fig. 7b are determined by integrating all downstream nitrogen containing species measured by FTIR (i.e., NO, NO$_2$, N$_2$O and NH$_3$). Thereby, for hydrogen conditions, a better catalyst performance is observed, regardless of its temperature. The conversion is always above 60% even at low temperatures and it increases up to over 95% for 320 °C. Under diesel conditions, a comparable temperature-dependent behavior occurs, but the conversion reaches only around 80%. At the lowest temperature of 220 °C, only a quarter of the stored NO can be converted. This may be due to using CO as the reductant, since its inferior regeneration behavior compared to hydrogen is already known in literature [24].

To evaluate the regeneration behavior not only the conversion is relevant, but also the amount of NO$_x$ converted into other harmful exhaust gases such as ammonia or nitrous oxide. The related selectivities shown in Fig. 8 are determined by the released amount of those gases relative to $m_{NO,max}$. Again, hydrogen conditions exhibit better catalyst performance due to the reduced formation of both NH$_3$ and N$_2$O.

Along with the improved conversion behavior at higher temperatures, selectivity towards harmful gases also decreases. Above 300 °C, NH$_3$ selectivity is below 10% in diesel operation and 3.5% at hydrogen conditions. Moreover, these amounts of ammonia could be stored and converted by a small passive SCR catalyst downstream of the NSC, and could therefore be used to reduce not converted NO$_x$ even better [46]. Far more problematic is the formation of nitrous oxide with its strong greenhouse impact. Even under hydrogen conditions, where N$_2$O selectivity is by far lower, up to 7% of the stored NO are still converted to nitrous oxide at the lowest tested temperature (220 °C). Nevertheless, N$_2$O selectivity drops significantly with increasing temperature to less than 0.3% at 375 °C. Overall, to prevent emission of harmful exhaust gases, regeneration temperatures of above 300 °C are preferred.

Finally, Fig. 9 compares the sensitivity of the RF-sensor to NO storage for the two engine conditions. Under

Fig. 7 **a** Maximum amount of NO stored in the catalyst relative to the catalyst volume; **b** proportion of previously stored NOx converted into non-harmful gases during regeneration

Fig. 8 Temperature-dependent selectivity of the NSC. Amount of NH_3 (**a**) or N_2O (**b**) released during regeneration in relation to the previously stored amount of NO
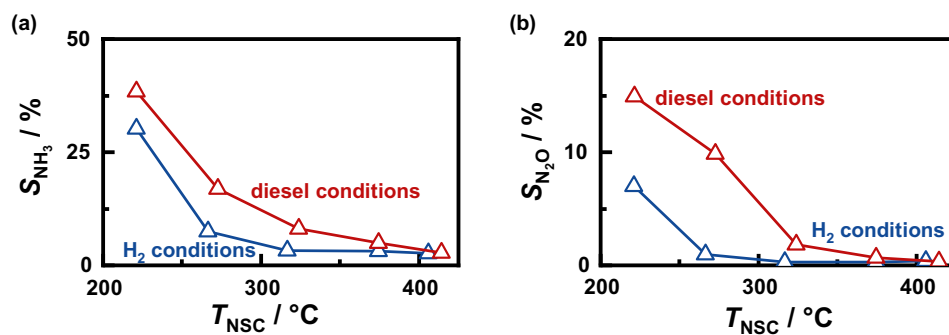
Fig. 9 Temperature-dependent shift of (**a**) the resonant frequency signal and (**b**) the quality factor relative to the stored NO
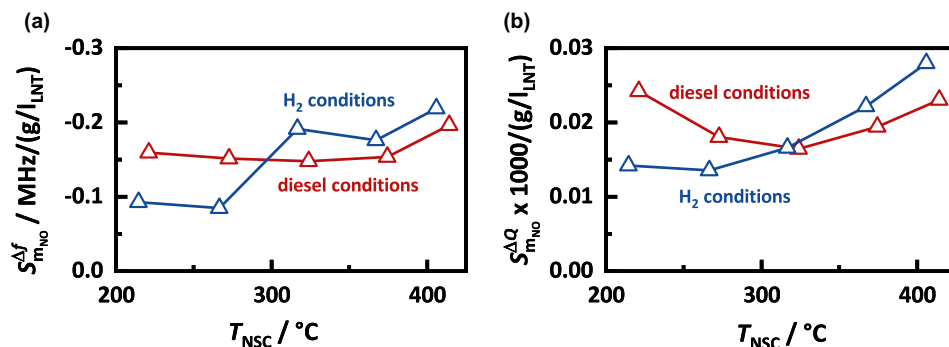
hydrogen conditions, a slightly higher sensitivity, both in terms of resonant frequency $S_{m_{NO}}^{\Delta f}$ and quality factor $S_{m_{NO}}^{\Delta Q}$, can be observed at high temperatures. At temperatures below 300 °C, however, there is a clear drop in sensitivity at the resonant frequency for hydrogen conditions, which was already clearly noticeable in Fig. 5. Under diesel conditions, on the other hand, the $S_{m_{NO}}^{\Delta f}$ shows almost no temperature sensitivity. With respect to the quality factor signal, an increase in sensitivity at higher temperature is evident, whereas under diesel conditions the sensitivity increases again at low temperatures. The reasons for the differences between both engine conditions were not analyzed further. In general, it is evident that the RF-sensor can detect the loading state of an NSC when operated with a hydrogen engine with a similar sensitivity as in combination with a diesel engine.

5 Conclusion

Hydrogen combustion engines can contribute to achieve CO_2-neutral mobility. However, zero emission operation cannot be achieved without exhaust aftertreatment systems, as nitrogen oxides may be formed due to high temperatures during combustion. With a NO_x storage catalyst, NO_x emissions could be reduced without additional reducing agents such as urea solutions in SCR systems.

In this work, it has been shown that an NSC operated under conditions typical for a hydrogen engine performs better than under those corresponding to a diesel engine.

In addition to higher NO_x storage capacity and better conversion rate, the formation of harmful by-products during regeneration such as NH_3 or N_2O was also reduced during hydrogen operation. In order to minimize these secondary emissions, NSCs should be preferably regenerated at temperatures not much lower than 300 °C. Nevertheless, the measurements also proved that, even at low exhaust gas temperatures of 200 °C, the storage capacity of NSCs is sufficient to buffer the very low NO_x emissions of a hydrogen ICE until regeneration at higher temperatures is possible.

To ensure emission-free operation, a permanent monitoring of the NO_x storage level is necessary to prevent breakthroughs of nitrogen oxides and to avoid too frequent regenerations. While previous work has already shown that the RF-sensor can be used to monitor the NO_x loading in diesel NSCs, this has now also been proven under the low CO_2 concentrations present in hydrogen applications. Furthermore, under rich conditions, a dependence between the resonant parameter shift and the air–fuel ratio could be found, which could possibly correlate with the oxidation degree of the NSC. Compared to diesel conditions, the RF-sensor shows a similar sensitivity with respect to NO loading. Thus, when operating with a hydrogen engine, the RF-sensor allows for a precise determination of the NO_x storage, similar as previously shown in [34] for diesel applications. If the air–fuel ratio is known during rich operation, it is also possible with the RF-sensor to determine the NO_x and O_2 storage during regeneration allowing a termination of the

regeneration before a breakthrough of reducing exhaust gas pollutants occur.

Since only loading with pure NO has been investigated so far, future work should also consider the influence of different NO/NO_2 mixtures. Furthermore, based on RF-sensor signals, a control system for ending regeneration automatically as soon as the NO_x storage is emptied would be conceivable. The evaluation of a possible advantage of the RF-sensor regarding the achievable conversion rate compared to the current used integrative determination using NO_x sensors should be carried out under realistic conditions on a transient test bench.

References

1. IPCC (2014) Summary for Policymakers. In: Edenhofer O, Pichs-Madruga R, Sokona Y et al. (eds) Climate change 2014: Mitigation of climate change Working Group III contribution to the Fifth Assessment Report of the Intergovernmental Panel on Climate Change. Cambridge University Press, Cambridge, United Kingdom and New York, NY, USA

2. Sims R, Schaeffer R, Creutzig F et al. (2014) Transport. In: Edenhofer O, Pichs-Madruga R, Sokona Y et al. (eds) Climate change 2014: Mitigation of climate change Working Group III contribution to the Fifth Assessment Report of the Intergovernmental Panel on Climate Change. Cambridge University Press, Cambridge, United Kingdom and New York, NY, USA

3. Sanguesa JA, Torres-Sanz V, Garrido P et al (2021) A review on electric vehicles: technologies and challenges. Smart Cities 4:372–404. https://doi.org/10.3390/smartcities4010022

4. ENTSO-E (2021) Position Paper on Electric Vehicle Integration into Power Grids

5. Un-Noor F, Padmanaban S, Mihet-Popa L et al (2017) A Comprehensive study of key electric vehicle (EV) components, technologies, challenges, impacts, and future direction of development. Energies 10:1217. https://doi.org/10.3390/en10081217

6. Stępień Z (2021) A comprehensive overview of hydrogen-fueled internal combustion engines: achievements and future challenges. Energies 14:6504. https://doi.org/10.3390/en14206504

7. Yamane K (2018) Hydrogen fueled ICE, successfully overcoming challenges through high pressure direct injection technologies: 40 years of Japanese Hydrogen ICE research and development. SAE Tech Pap. https://doi.org/10.4271/2018-01-1145

8. Staffell I, Scamman D, Velazquez Abad A et al (2019) The role of hydrogen and fuel cells in the global energy system. Energy Environ Sci 12:463–491. https://doi.org/10.1039/C8EE01157E

9. Verhelst S (2014) Recent progress in the use of hydrogen as a fuel for internal combustion engines. Int J Hydrog Energy 39:1071–1085. https://doi.org/10.1016/j.ijhydene.2013.10.102

10. Caton PA, Pruitt JT (2009) Homogeneous charge compression ignition of hydrogen in a single-cylinder diesel engine. Int J Engine Res 10:45–63. https://doi.org/10.1243/14680874JER02208

11. Lewis AC (2021) Optimising air quality co-benefits in a hydrogen economy: a case for hydrogen-specific standards for NO_x emissions. Environ Sci Atmos 1:201–207. https://doi.org/10.1039/D1EA00037C

12. Ma D-S, Sun ZY (2020) Progress on the studies about NO_x emission in PFI-H_2ICE. Int J Hydrog Energy 45:10580–10591. https://doi.org/10.1016/j.ijhydene.2019.11.065

13. Sterlepper S, Fischer M, Claßen J et al (2021) Concepts for hydrogen internal combustion engines and their implications on the exhaust gas aftertreatment system. Energies 14:8166. https://doi.org/10.3390/en14238166

14. Krishnanunni J, Bhatia D, Dutta V et al (2019) Power improvement and NO_x reduction strategies for a hydrogen-fueled multicylinder internal combustion engine. J Eng Gas Turbines Power. https://doi.org/10.1115/1.4044966

15. Johnson TV (2015) Review of vehicular emissions trends. SAE Int J Engines 8:1152–1167. https://doi.org/10.4271/2015-01-0993

16. Borchers M, Keller K, Lott P et al (2021) Selective Catalytic reduction of NO_x with H_2 for cleaning exhausts of hydrogen engines: impact of H_2O, O_2, and NO/H_2 ratio. Ind Eng Chem Res 60:6613–6626. https://doi.org/10.1021/acs.iecr.0c05630

17. Resitoglu IA, Keskin A (2017) Hydrogen applications in selective catalytic reduction of NO_x emissions from diesel engines. Int J Hydrog Energy 42:23389–23394. https://doi.org/10.1016/j.ijhydene.2017.02.011

18. Savva PG, Costa CN (2011) Hydrogen Lean-DeNO_x as an alternative to the ammonia and hydrocarbon selective catalytic reduction (SCR). Catal Rev 53:91–151. https://doi.org/10.1080/01614940.2011.557964

19. Koch DT, Sousa A, Bertram D (2019) H_2-engine operation with EGR Achieving high power and high efficiency emission-free combustion. SAE Tech Pap. https://doi.org/10.4271/2019-01-2178

20. Roy S, Baiker A (2009) NO_x storage-reduction catalysis: from mechanism and materials properties to storage-reduction performance. Chem Rev 109:4054–4091. https://doi.org/10.1021/cr800496f

21. Ji Y, Toops TJ, Crocker M (2007) Effect of ceria on the storage and regeneration behavior of a model lean NO_x trap catalyst. Catal Lett 119:257–264. https://doi.org/10.1007/s10562-007-9226-2

22. AL-Harbi M, Epling WS (2009) Investigating the effect of NO versus NO_2 on the performance of a model NO_x storage/reduction catalyst. Catal Lett 130:121–129. https://doi.org/10.1007/s10562-009-9912-3

23. Epling WS, Campbell LE, Yezerets A et al (2004) Overview of the fundamental reactions and degradation mechanisms of NOx storage/reduction catalysts. Catal Rev 46:163–245. https://doi.org/10.1081/CR-200031932

24. Poulston S, Rajaram RR (2003) Regeneration of NOx trap catalysts. Catal Today 81:603–610. https://doi.org/10.1016/S0920-5861(03)00158-5

25. Rottengruber H, Wiebicke U, Woschni G et al (2000) Wasserstoff-dieselmotor mit direkteinspritzung, hoher leistungsdichte und geringer abgasemission. MTZ Motortech Z 61:122–128. https://doi.org/10.1007/BF03226557

26. Lietti L, Nova I, Forzatti P (2008) Role of ammonia in the reduction by hydrogen of NO$_x$ stored over Pt–Ba/Al$_2$O$_3$ lean NO$_x$ trap catalysts. J Catal 257:270–282. https://doi.org/10.1016/j.jcat.2008.05.005

27. Lietti L, Forzatti P, Nova I et al (2001) NO$_x$ storage reduction over Pt-Ba/γ-Al$_2$O$_3$ catalyst. J Catal 204:175–191. https://doi.org/10.1006/jcat.2001.3370

28. Asik JR (2000) Closed loop control of lean NOx traps. In: Krüger S, Gessner W (eds) Advanced microsystems for automotive applications 2000. Springer, Heidelberg

29. Karimshoushtari M, Novara C, Trotta A (2017) Data-driven model predictive control for lean NO$_x$ trap regeneration. IFAC-PapersOnLine 50:6004–6009. https://doi.org/10.1016/j.ifacol.2017.08.1436

30. Vitesco Technologies (2021) Building an electrification powerhouse—our solutions. Technical Information

31. Moos R, Beulertz G, Reiß S et al (2013) Overview: status of the microwave-based automotive catalyst state diagnosis. Top Catal 56:358–364. https://doi.org/10.1007/s11244-013-9980-x

32. Moos R, Rauch D, Votsmeier M et al (2016) Review on radio frequency based monitoring of SCR and three way catalysts. Top Catal 59:961–969. https://doi.org/10.1007/s11244-016-0575-1

33. Fremerey P, Reiß S, Geupel A et al (2011) Determination of the NO$_x$ Loading of an Automotive lean NO$_x$ trap by directly monitoring the electrical properties of the catalyst material itself. Sensors 11:8261–8280. https://doi.org/10.3390/s110908261

34. Walter S, Ruwisch L, Göbel U et al (2019) Radio frequency-based determination of the oxygen and the NO$_x$ storage level of NO$_x$ storage catalysts. Top Catal 62:157–163. https://doi.org/10.1007/s11244-018-1079-y

35. Rauch D, Dietrich M, Simons T et al (2017) Microwave cavity perturbation studies on H-form and Cu Ion-exchanged SCR catalyst materials: correlation of ammonia storage and dielectric properties. Top Catal 60:243–249. https://doi.org/10.1007/s11244-016-0605-z

36. Dietrich M, Rauch D, Porch A et al (2014) A laboratory test setup for in situ measurements of the dielectric properties of catalyst powder samples under reaction conditions by microwave cavity perturbation: set up and initial tests. Sensors 14:16856–16868. https://doi.org/10.3390/s140916856

37. Steiner C, Walter S, Malashchuk V et al (2020) Determination of the dielectric properties of storage materials for exhaust gas aftertreatment using the microwave cavity perturbation method. Sensors 20:6024. https://doi.org/10.3390/s20216024

38. Saji K, Kondo H, Takeuchi T et al (1988) Voltage step characteristics of oxygen concentration cell sensors for nonequilibrium gas mixtures. J Electrochem Soc 135:1686–1691. https://doi.org/10.1149/1.2096097

39. Dietrich M, Jahn C, Lanzerath P et al (2015) Microwave-based oxidation state and soot loading determination on gasoline particulate filters with three-way catalyst coating for homogenously operated gasoline engines. Sensors 15:21971–21988. https://doi.org/10.3390/s150921971

40. Liu Y, Zheng Y, Harold MP et al (2013) Lean NO$_x$ reduction with H$_2$ and CO in dual-layer LNT–SCR monolithic catalysts: impact of ceria loading. Top Catal 56:104–108. https://doi.org/10.1007/s11244-013-9936-1

41. Steiner C, Gänzler AM, Zehentbauer M et al (2018) Oxidation state and dielectric properties of ceria-based catalysts by complementary microwave cavity perturbation and x-ray absorption spectroscopy measurements. Top Catal 85:595. https://doi.org/10.1007/s11244-018-1110-3

42. Beulertz G, Fritsch M, Fischerauer G et al (2013) Microwave cavity perturbation as a tool for laboratory in situ measurement of the oxidation state of three way catalysts. Top Catal 56:405–409. https://doi.org/10.1007/s11244-013-9987-3

43. Müller SA, Degler D, Feldmann C et al (2018) Exploiting synergies in catalysis and gas sensing using noble metal-loaded oxide composites. Chem Cat Chem 10:864–880. https://doi.org/10.1002/cctc.201701545

44. Fridell E, Skoglundh M, Westerberg B et al (1999) NO$_x$ storage in barium-containing catalysts. J Catal 183:196–209. https://doi.org/10.1006/jcat.1999.2415

45. Kobayashi T, Yamada T, Kayano K (1997) Study of NOx trap reaction by thermodynamic calculation. SAE Tech Pap. https://doi.org/10.4271/970745

46. Weibel M, Waldbüßer N, Wunsch R et al (2009) A novel approach to catalysis for NO$_x$ reduction in diesel exhaust gas. Top Catal 52:1702–1708. https://doi.org/10.1007/s11244-009-9329-7